Identification of key ferroptosis-related genes associated with the development of gastric cancer: Prognostic models, molecular mechanisms and potential treatment strategies

HUI WANG[1,2*], HANG CHEN[1*], JIANJUN LIU[3], DAN ZHANG[1], DA WANG[1], MINSHAN HUANG[1], MENGWEI LI[1], SUYU HE[2] and LANQING MA[1]

[1]Department of Gastroenterology, The First Affiliated Hospital, Yunnan Institute of Digestive Disease, Yunnan Clinical Research Center for Digestive Diseases, Kunming Medical University, Kunming, Yunnan 650032, P.R. China; [2]The Fourth Department of Digestive Disease Center, Suining Central Hospital, Suining, Sichuan 629099, P.R. China; [3]Academy of Biomedical Engineering, Kunming Medical University, Kunming, Yunnan 650500, P.R. China

Received December 19, 2024; Accepted June 6, 2025

DOI: 10.3892/ol.2025.15196

Abstract. Ferroptosis is a novel iron-dependent form of cell death that influences the development and progression of gastric cancer (GC), affecting its growth, invasion and metastasis. However, molecular regulatory mechanisms of ferroptosis in GC remain unclear. The present study aimed to identify key ferroptosis-related genes associated with GC development. Ferroptosis-related genes were collected from FerrDb, a database that collects data on genes and substances that regulate ferroptosis, and the top survival-related genes (including progression-free and overall survival), and differentially expressed genes were identified using data from The Cancer Genome Atlas stomach adenocarcinoma (STAD) samples. Following intersection analysis, least absolute shrinkage and selection operator analysis was performed on 140 screened important genes, and 14 key ferroptosis-related genes in STAD were obtained using Cox regression models. By reviewing the expression of these genes through the Gene Set Cancer Analysis tool and their correlation with survival, the present study analyzed their overall role in STAD. Tumor immunity analysis was performed to identify potential microRNAs (miRs) and drugs targeting key carcinogenic ferroptosis genes in STAD. NADPH oxidase (NOX) 4, NOX5, aldo-keto reductase family 1 member C2, RNA binding motif single stranded interacting protein 1 (RBMS1), GABA type A receptor associated protein like 2 (GABARAPL2), gap junction protein α1 (GJA1), transferrin and hydroxycarboxylic acid receptor 1 were notable risk genes. Additionally, by examining the association between these genes and tumor-infiltrating immune cells, it was discovered that GABARAPL2, GJA1, NOX4 and RBMS1 may influence the immune microenvironment. In total, five miRs [*Homo sapiens* (hsa)-miR-6795-5p, hsa-miR-6758-5p, hsa-miR-501-5p, hsa-miR-505-5p and hsa-miR-484] with potential therapeutic implications for STAD were identified as targeting carcinogenic genes. Finally, using the Genomics of Drug Sensitivity in Cancer and Cancer Therapeutics Response Portal databases, potential drugs [(5Z)-7-oxozeaenol, selumetinib, RDEA119, AZ628, dabrafenib and trametinib] were identified based on the aforementioned seven key carcinogenic genes, focusing on those that targeted multiple genes. In conclusion, the present study identified 14 key ferroptosis-related genes, and seven key carcinogenic genes, which represent promising novel molecular targets for the prognosis and treatment of GC.

Introduction

Currently, gastric cancer (GC) is one of the most common cancer types and the leading cause of cancer-associated mortality worldwide (1-6). According to the 2020 global cancer statistics, GC) remained a significant global health burden in 2020, causing 10.89 million new cancer cases and 7.69 million deaths worldwide. This positioned it as the fifth most common malignancy and the fourth leading cause of cancer-related mortality (7). In the early stages, GC-associated symptoms are unclear or absent. In the majority of cases, it has progressed to a stage that is not amenable to radical surgery at the time of diagnosis. In most cancer databases, GC is labeled stomach adenocarcinoma (STAD) because, in 95% of GC cases, this is the predominant histological subtype of gastrointestinal malignancy (8). To date, therapeutic outcomes for STAD remain limited, with a 5-year overall survival (OS) rate <10% in patients with advanced STAD (9). Recurrence is common even after resection (10). Therefore, the identification

Correspondence to: Dr Lanqing Ma, Department of Gastroenterology, The First Affiliated Hospital, Yunnan Institute of Digestive Disease, Yunnan Clinical Research Center for Digestive Diseases, Kunming Medical University, 295 Xichang Road, Kunming, Yunnan 650032, P.R. China
E-mail: malanqing@kmmu.edu.cn

*Contributed equally

Key words: ferroptosis, gastric cancer, stomach adenocarcinoma, prognostic model, tumor immunity

of new biomarkers is key for guiding systemic treatment strategies. This highlights the urgency of developing an accurate prognostic model and novel therapeutic targets for patients with STAD.

Ferroptosis is a type of iron-dependent programmed cell death that is distinct from apoptosis, necrosis and autophagy. The primary mechanism is the catalysis of lipid peroxidation of unsaturated fatty acids highly expressed on the cell membrane in the presence of divalent iron or ester oxygenase, which induces cell death. This results in a decrease in the regulation of the antioxidant system (glutathione system) (11-17). It is hypothesized that ferroptosis is associated with the occurrence and development of tumors, such as liver and gastric cancer (12,18-21). The association between ferroptosis and GC has also been increasingly recognized (22-36), and ferroptosis is hypothesized to serve a vital role in GC development and progression (37,38). Thus, targeting ferroptosis may be a potential therapeutic strategy for patients with GC.

Ferroptosis is a double-edged sword in gastrointestinal disease, since the inhibition of ferroptosis relieves the symptoms of intestinal injury, and the induction of ferroptosis via pharmacological agonists or bioactive compounds inhibits the proliferation of GC (32). Ferroptosis inducers affect different steps in ferroptosis to regulate GC proliferation, invasion and metastasis, although development of drug resistance in GC cells poses a hurdle (23). However, limitations exist in previous studies (23,31,39-41). Firstly, the efficacy of the prognostic models for GC based on ferroptosis-related genes is poor, as demonstrated by the fact that the log-rank P-values in the prognostic models are often not low enough (P>0.01), the hazard ratios of high- vs. low-risk are not high enough and the optimal area under the curve (AUC) values of the receiver operating characteristic (ROC) curves are often ~0.7 (39) . Secondly, considering the dual nature of ferroptosis, its role in GC progression remains controversial, and needs to be clarified with more evidence. Thirdly, the roles of numerous important drivers and suppressors [solute Carrier Family 7 Member 11 (SLC7A11)/Glutathione Peroxidase 4 (GPX4)] of ferroptosis in GC progression remain unclear. Finally, novel therapeutic strategies based on targeting ferroptosis, including potential small molecule drugs and microRNAs (miRNAs or miRs) as molecular drugs to regulate gene expression, remain to be explored.

The present study aimed to identify key ferroptosis-related genes associated with the development of GC to construct prognostic models and identify new molecular mechanisms and potential treatment strategies. The present findings may serve as a reference for future studies on the mechanism underlying ferroptosis and treatment of GC.

Materials and methods

Key gene screening and survival prediction via the Cox regression model. Ferroptosis-related genes were collected from FerrDb (zhounan.org/ferrdb/current/), which is an open-source, open access, manually curated and continuously updated database (Fig. 1). There were 12 ferroptosis markers, 369 ferroptosis driver items and 348 ferroptosis suppressor (or inhibitor) items. Following deduplication, 484 ferroptosis-related genes remained. Subsequently, using the Gene Expression Profiling Interactive Analysis 2 database(gepia.cancer-pku.cn/), the 500 top OS- and progression-free survival (PFS)-associated genes were identified, and 910 survival-related genes were identified following deduplication. In addition, there were 4,640 differentially expressed genes (DEGs) between STAD and adjacent normal tissue. The intersection of these three sets was analyzed, and three common elements were found in addition to 124 STAD-ferroptosis genes and 13 survival-ferroptosis genes. These 140 genes were used to establish the prognostic models.

For OS and PFS prediction, two multivariate Cox regression models were established based on gastric cancer (STAD) samples from The Cancer Genome Atlas (TCGA; Project ID: TCGA-STAD; Data Portal: https://portal.gdc.cancer.gov/), as described in the original pan-cancer analysis by TCGA Research Network (42). Least absolute shrinkage and selection operator (LASSO) regression algorithm was used for feature selection using 10-fold cross-validation and nine features were selected. The equations of the Cox regression models were calculated as risk scores, and patients were divided into high- and low-risk groups using the median value as the cutoff (1.85). The log-rank test was used to compare differences in survival between the high- and low-risk groups. For the Kaplan-Meier curves, the P-values and hazard rations (HRs) with 95% confidence intervals (CIs) were generated using log-rank tests. ROC curves with AUC values were constructed to assess the efficacy of the Cox regression models. The key features (genes) of the models were collected, and aggregated into the key gene set. As the performance of OS was still not satisfactory (as the aim was to reduce the likelihood ratio test and the log-rank P-value to $<1x10^{-12}$), another Cox regression model was constructed after the key genes were obtained using the Tumor Immune Estimation Resource (TIMER) database (timer2.compbio.cn/timer1/). The model incorporated demographic and clinical features(age, tumor stage) , and removed certain unimportant gene expression features(MYB, PRP5) to ensure that the log-rank P-value was $<1x10^{-12}$.

Roles of key genes in STAD. For each key ferroptosis gene in STAD, the expression between tumor and adjacent normal tissue was compared. The expression trends from stages I to IV were acquired via the Gene Set Cancer Analysis (GSCA) online tool (guolab.wchscu.cn/GSCA/#/). Using the same tool (based on the TCGA datasets), the association between gene expression and different types of survival [disease-specific survival (DSS), OS and PFS] were presented in a bubble plot (where red indicates increased risk). Additionally, the association between key gene expression levels and the activation/inhibition of important pathways in cancer development were using the GSCA tool.

Key-gene interaction networks. Using the GeneMANIA online tool (genemania.org/), the interaction networks between 14 key genes were explored by focusing on genetic and physical protein interactions and co-expression.

Tumor immunity analysis based on key ferroptosis genes in STAD. Using the TIMER database, the immune characteristics of the cells were evaluated. Correlation between key ferroptosis genes in STAD and tumor-infiltrating immune cells was determined using Pearson's coefficient. The present

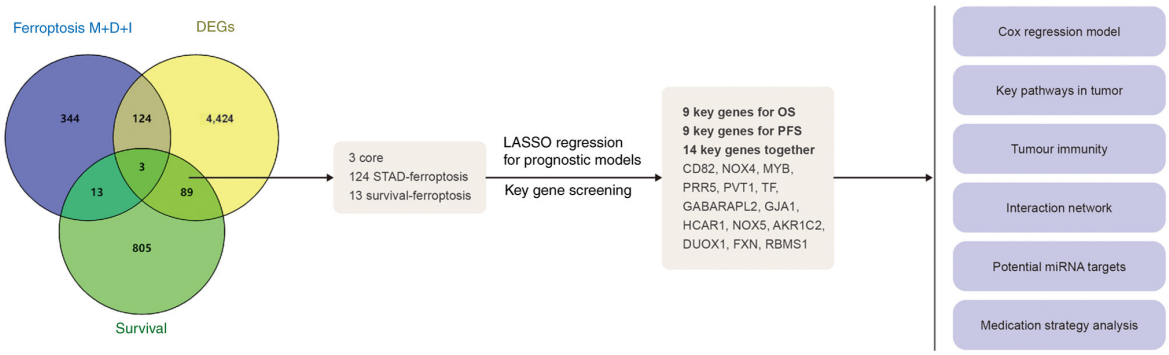

Figure 1. Flow chart of the present study. A total of 140 key ferroptosis-related genes were obtained, and 14 key genes were screened by LASSO and prognostic models for the following analyses: i) Optimized Cox regression model, ii) key pathway analysis in tumors, iii) immunity analysis and iv) identification of potential miRNAs and drug targeting key carcinogenic ferroptosis genes in STAD. M, marker; D, driver; I, inhibitor; LASSO, least absolute shrinkage and selection operator regression; miRNA, microRNA; STAD, stomach adenocarcinoma; DEG, differentially expressed gene; OS, overall survival; PFS, progression-free survival; NOX, NADPH oxidase; MYB, MYB proto-oncogene, transcription factor; PRR5, proline-rich protein 5; PVT1, Pvt1 oncogene; TF, transferrin; GABARAPL2, GABA type A receptor-associated protein-like 2; GJA1, gap junction protein α1; HCAR1, hydroxycarboxylic acid receptor 1; AKR1C2, aldo-keto reductase family 1 member C2; DUOX1, dual oxidase 1; FXN, frataxin; RBMS1, RNA binding motif single stranded interacting protein 1.

study focused only on immune cells with expression of key ferroptosis genes >0.3 (P<0.001).

Potential miRNAs that target key carcinogenic ferroptosis genes in STAD. Among the 14 key ferroptosis genes, the carcinogenic genes in STAD were selected according to the following criteria: i) Coefficient in the prognostic equation should be >0.05 (for either PFS or OS) and ii) expression tendency should be in increasing order from stage I to IV or significant risk factors for OS and PFS (univariate analysis). Overall, seven genes were regarded as key carcinogenic ferroptosis genes in STAD. Using the miRWalk database(mirwalk.umm.uni-heidelberg.de/), the miRNAs targeting these seven genes were downloaded. The miRNAs with the most matching pairs (base-pairing sequences with the seven genes) and the greatest number of target genes were considered to have a potential therapeutic value.

Potential drugs based on key ferroptosis genes in STAD. The GSCA tool was used to identify potential drugs for treating STAD. Genomics of Drug Sensitivity in Cancer (GDSC) and Cancer Therapeutics Response Portal (CTRP) databases (cancerrxgene.org/; portals.broadinstitute.org/ctrp/) were used to obtain the half-maximal inhibitory concentration (IC_{50}) values of the drugs. The drugs were ranked by the integrated level of the correlation coefficient and false discovery rate values, and the top 30 ranked drugs were shown in bubble plots. In addition, theoretically, if IC_{50} is significantly negatively correlated with a greater number of carcinogenic mRNAs, this suggests a greater likelihood that the drug will exert an anti-STAD effect.

Human tissue collection. The tumors and surrounding normal tissue (distance, 3-5 cm from the tumor tissue) of 20 patients (12 males and 8 females, aged 18-60 years) with GC who underwent surgical resection in The First Affiliated Hospital of Kunming Medical University (Kunming, China) from April to July 2024 were collected. The inclusion criteria were as follows: i) Patients diagnosed with GC by pathological examination; ii) aged ≥18 years and ≤60 years; iii) received tumor resection surgery; iv)did not receive preoperative chemotherapy, radiotherapy, biotherapy or traditional Chinese medicine; and v) followed the normal follow-up requirements. In addition, the exclusion criteria were as follows: i) Patients with other primary types of cancer; ii) with needle or blood phobia; and iii) pregnant women or lactating mothers. The present study was approved by The First Affiliated Hospital of Kunming Medical University Ethics Committee (approval no. 2024 lunshen L no. 78). All samples were obtained with written informed consent obtained from patients, and the study adhered to the ethical principles of the Declaration of Helsinki.

Cell culture and transfection. The GC cell line AGS was purchased from American Type Culture Collection and cultured in RPMI-1640 medium (Procell) supplemented with 10% fetal bovine serum (Procell) and 1% penicillin/streptomycin in 5% CO_2 in a humidified atmosphere at 37˚C. Following 24 h culture, the *Homo sapiens* (hsa)-miR-501-5p inhibitor (delivered as siRNA) and hsa-miR-484 mimic were transfected separately, along with their respective negative controls, using Lipofectamine 3000 (Invitrogen, Thermo Fisher Scientific), and incubated. The concentrations used were 50 nM for miR-484 mimic and 100 nM for miR-501-5p siRNA. Transfection was carried out at 37˚C for 6 h. Cells were harvested 48 h post-transfection for subsequent assays. hsa-miR-484 mimic, hsa-miR-501-5p inhibitor (siRNA format) and non-targeting scrambled negative controls were designed and synthesized by Shanghai GeneChem Co., Ltd. The sequences were as follows: miR-484 mimic: Forward, 5'-UCAGGCUCAGUCCCCUCCCGAU-3' and R:5'-CGGGAGGGGACUGAGCCUGAGC-3' and mimic negative controls: Forward, 5'-UUGUACUACACAAAAGUACUG-3' and reverse, 5'-GUACUUUUGUGUAGUACAAGC-3'; miR-501-5p siRNA: F:5'-UCUCACCCAGGGACAAAGGA-3' and R:5'-UCCUUUGUCCCUGGGUGAGA-3' and siRNA negative controls: F:5'-UUCUCCGAACGUGUCACGUUU-3' and R:5'-ACGUGACACGUUCGGAGAAUU-3'.

Reverse transcription-quantitative PCR (RT-qPCR). TRIzol® was used to isolate RNA from GC cell lines and tissue.

According to the manufacturer's instructions, cDNA was synthesized from RNA using a PrimeScript™ RT reagent kit (Takara). TB Green® Premix Ex Taq™ II FAST qPCR kit (Takara) was used for qPCR. qPCR was performed using the following thermocycling conditions: Initial denaturation at 95˚C for 3 min, followed by 45 cycles of 95˚C for 5 sec and 60˚C for 30 sec. The amplification of DNA was performed with TB Green® Premix Ex Taq (Takara). CFX96™ Real-Time System was used to evaluate the amplification of each gene. The primer sequences were as follows: hsa-miR-501-5p: forward: 5'-AUC CUUUGUCCCUGGGUGAGA-3' and reverse: 5'-GTGCAG GGTCCGAGGT-3'; hsa-miR-484: Forward: 5'-UCAGGCUCA GUCCCCUCCCGAU-3' and reverse: 5'-GTGCAGGGTCCG AGGT-3' and U6 sense: Forward: 5'-CTCGCTTCGGCAGCA CA-3' and reverse: 5'-AACGCTTCACGA ATTTGCGT-3'. The miRNA primers were provided by Tiangen Biotech Co., Ltd. U6 was used as an endogenous control. The results were determined using the $2^{-\Delta\Delta Cq}$ method (43). All the experiments were repeated three times.

Cell viability assay. GC AGS cells were treated with DMSO, (5Z)-7-oxozeanol (0, 1, 2, 4 μmol/l), selumetinib (0, 12.5, 25, 50 μmol/l), RDEA119 (0, 5, 50, 100 μmol/l), AZ628 (0, 0.5, 1, 1.5 μmol/l), dabrafenib(0, 0.25, 0.5, 1 μmol/l) or trametinib (0, 0.5, 5, 50 μmol/l) (all MedChemExpress) for 0, 24, 48 or 72 h, 37˚C. Following digestion with trypsin, the total number of cells was counted on a cell counting plate. RPMI-1640 (Procell) containing 5,000 AGS cells was added to each well of a 96-well plate. Cell Counting Kit-8 assay (Beyotime Institute of Biotechnology) was used to observe the proliferative capacity (incubation for 2 h). Absorbance values of the cells at 450 nm were determined. All the experiments were repeated three times.

Western blotting. Cell Lysis buffer (Cell Signaling Technology) containing PMSF (1 mM, Beyotime Institute of Biotechnology) was used to lyse AGS cells. The BCA method was used to determine the protein concentration. After that, the protein samples (20 μg/lane) were separated using 8-12% sodium dodecyl sulfate-polyacrylamide gel electrophoresis gels, and transferred to polyvinylidene difluoride membranes (MilliporeSigma), which were incubated for 2 h in 5% skimmed milk at 25˚C. Subsequently, primary antibodies were added overnight at 4˚C. Following 2 h incubation with the secondary antibody at 25˚C, the membranes were washed three times with TBS-Tween 20 (0.1%), and ECL (cat. no. WBULS0100; Millipore) was added to the membrane, which was placed on a GelDoc imaging system. ImageJ software (v1.54f, https://imagej.net/ij/) was used to analyze the optical density. The antibodies were as follows: Anti-aldo-keto reductase family 1 member C2 (AKR1C2; 1:200; cat. no. 13035; Cell Signaling Technology, Inc.), anti-transferrin (TF; 1:500; cat no. 17435-1-AP; Proteintech Group, Inc.), anti-NADPH oxidase (NOX) 4 (1:500; cat. no. 14347-1-AP; Proteintech Group, Inc.), anti-RNA binding motif single stranded interacting protein 1 (RBMS1; 1:400; cat. no. ab150353; Abcam), anti-β-actin (1:2,000; cat. no. 66009-1-Ig; Proteintech Group, Inc.) and HRP-conjugated goat anti-mouse IgG (1:1,000; cat. no. D110087; Sangon Biotech Co., Ltd.). β-actin was used as a loading control for normalization. All the experiments were repeated three times.

Statistical analysis. GraphPad Prism 8.0 (GraphPad; Dotmatics) or SPSS 26.0 (IBM Corp.) statistical software were used to analyze the data. Kolmogorov-Smirnov test was used to assess normal distribution. Data conforming to a normal distribution are presented as the mean ± standard deviation. Paired samples were compared with paired Student's t-test. Comparisons of >2 groups were made with one-way ANOVA followed by Dunnett's test. $P<0.05$ was considered to indicate a statistically significant difference. Each experiment was independently repeated three times.

Results

Key ferroptosis genes in STAD and prognostic models. The intersection analysis of 484 ferroptosis- and 910 survival-related genes and 4,640 DEGs in STAD revealed that 140 genes were notable ferroptosis genes in STAD. Using the 140 key genes, the LASSO regression algorithm was used for feature selection, and two Cox regression models for OS and FPS were generated.

For OS prediction (Fig. 2), the regression model was as follows: Risk score=(-0.0065) x CD82 + (0.08) x NOX4 + (-0.0219) x MYB proto-oncogene, transcription factor (MYB) + ($-6x10^{-4}$) x proline rich protein 5 (PRR5) + (-0.026) x Pvt1 oncogene (PVT1) + (0.1876) x GABA type A receptor associated protein like 2 (GABARAPL2) + (0.0711) x gap junction protein α1 (GJA1) + (0.0086) x hydroxycarboxylic acid receptor 1 (HCAR1) + (0.5351) x NOX5. This model contained nine features (Fig. 2A-C), among which, NOX4, NOX5, GABARAPL2 and GJA1 were the most important risk factors. It had satisfactory efficacy in terms of 5-6-year survival (AUC >0.72; Fig. 2D). The HR of the high-risk group was 2.66 (Fig. 2D). The additional OS prediction model was constructed using seven genes(CD82, NOX4, PVT1, GABARAPL2, TF, HCAR1and NOX5) along with several clinical features (age, tumor stage; Fig. 2E), and validated its performance using standard Kaplan-Meier curves and ROC curves (Fig. 2F-G). Kaplan-Meier curves stratified patients into prognostically distinct risk groups (log-rank $P<0.0001$), with the low-risk group exhibiting a median survival time (6.02 years) four times longer than that of the high-risk group (1.51 years). All high-risk patients died within 5 years, whereas low-risk patients demonstrated sustained survival with cases remaining alive at the 10-year mark (Fig. 2F). ROC analysis confirmed the model's robust discriminative ability from 1 to 9 years (all AUC >0.70), with peak predictive performance at 6 years (AUC=0.787, 95% CI: 0.620-0.954). Strong predictive validity was also maintained at 1 (AUC=0.713) and 2 years (AUC=0.751), highlighting its utility for both short- and long-term survival prediction (Fig. 2G).

For PFS prediction (Fig. 3), the regression model was as follows: Risk score=(-0.0907) x AKR1C2 + (0.0074) x dual oxidase 1 + (-0.0384) x MYB + (-0.0483) x frataxin (FXN) + (0.118) x RBMS1 + (0.0132) x GABARAPL2 + (0.0883) x TF + (0.066) x HCAR1 + (0.7408) x NOX5. This model also had nine features (Fig. 3A-C), among which, AKR1C2, RBMS1, NOX5, GABARAPL2, TF and HCAR1 were the

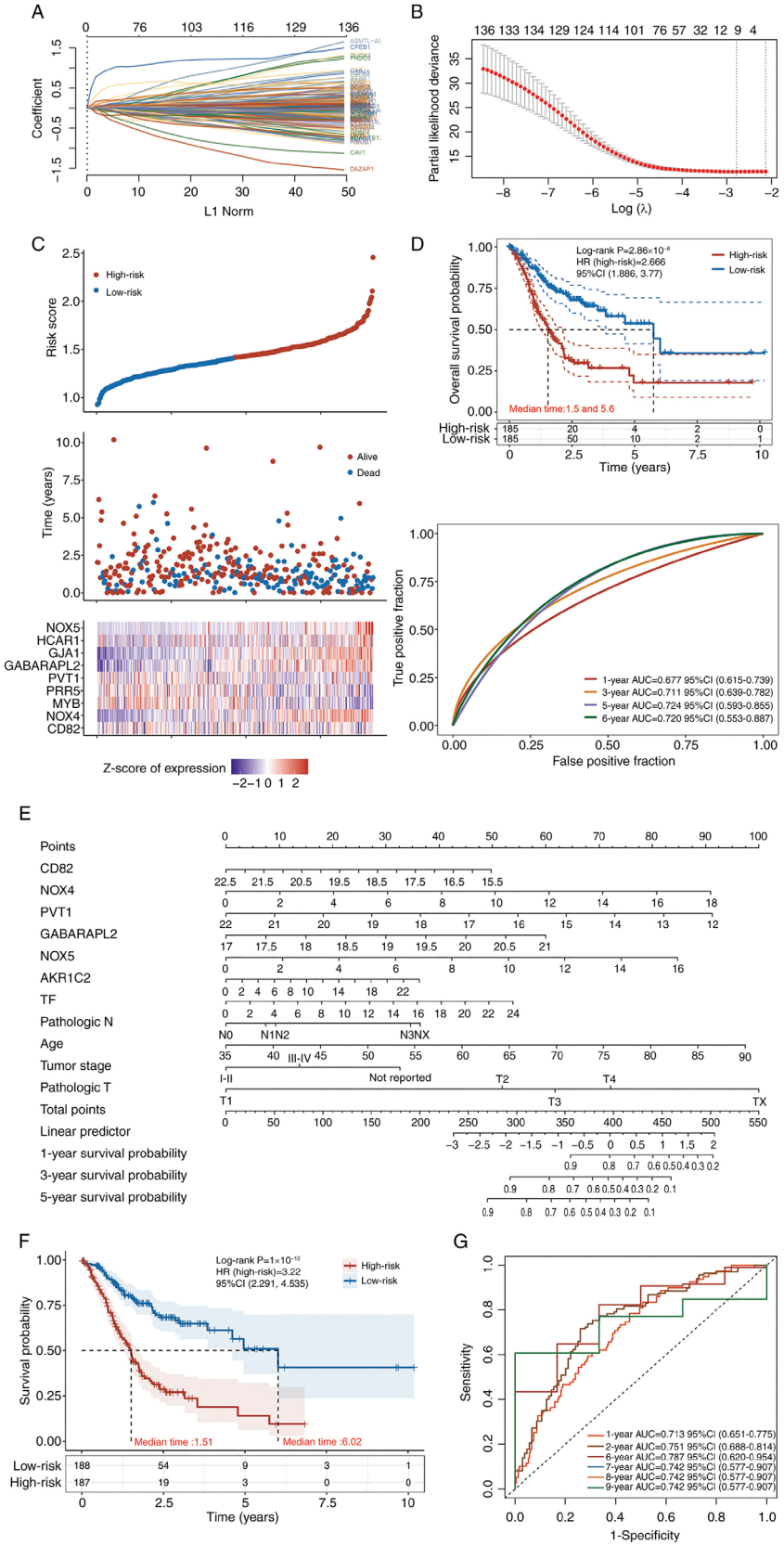

Figure 2. LASSO analysis and Cox regression models for OS prediction. (A) Coefficients of the selected features are shown by the λ parameter, where the horizontal coordinate represents the value of the independent variable λ and the vertical coordinate represents the coefficients of the independent variables. (B) Partial likelihood deviance plotted against log(λ) values calculated through the LASSO Cox regression model. (C) Association between expression of nine key genes in patients with gastric adenocarcinoma from The Cancer Genome Atlas database with patient risk scores and survival times. (D) Median OS time of the low- and high-risk groups, and receiver operating characteristic curve of the Cox regression model for the prediction of OS. (E-G) Cox regression models constructed with the key genes from TIMER database. (E) Nomogram of the constructed COX regression model, visually presenting the model; (F) KM curve of the model; (G) ROC curve of the model. LASSO, least absolute shrinkage and selection operator; OS, overall survival; HR, hazard ratio; AUC, area under the curve; CI, confidence interval; NOX, NADPH oxidase; MYB, MYB proto-oncogene, transcription factor; PRR5, proline rich protein 5; PVT1, Pvt1 oncogene; GABARAPL2, GABA type A receptor associated protein like 2; GJA1, gap junction protein α1; HCAR1, hydroxycarboxylic acid receptor 1.

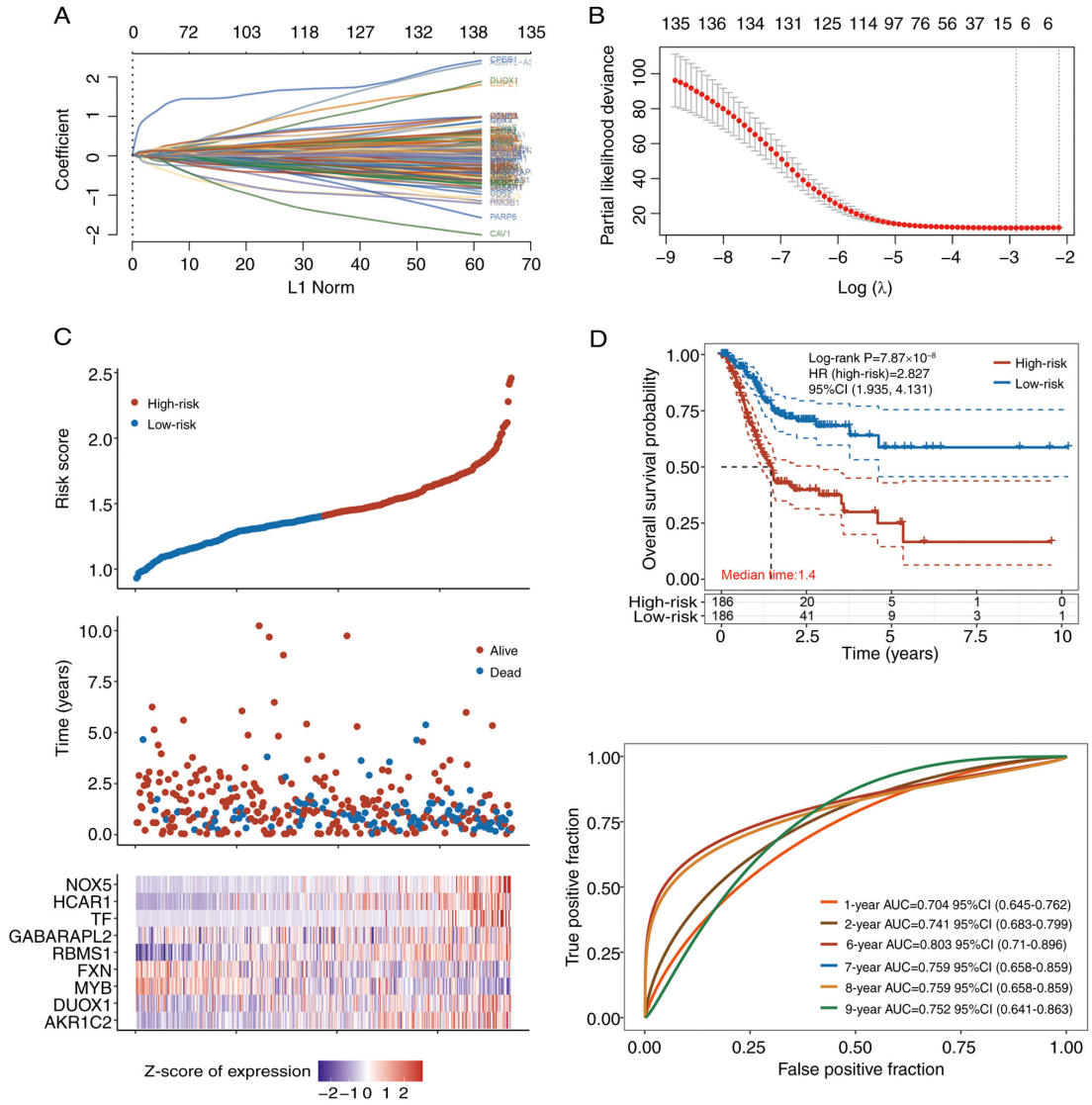

Figure 3. LASSO analysis and Cox regression models for PFS prediction. (A) Coefficients of the selected features are shown by the λ parameter, with the horizontal coordinate representing the value of the independent variable λ and the vertical coordinate representing the coefficients of the independent variables. (B) Partial likelihood deviance plotted against log(λ) values calculated via the LASSO Cox regression model. (C) Associations between risk scores and survival times of patients with expressing nine key genes in patients with stomach adenocarcinoma from The Cancer Genome Atlas database. (D) Median PFS of the low- and high-risk groups, and receiver operating characteristic curve of the Cox regression model for the prediction of PFS. LASSO, least absolute shrinkage and selection operator; PFS, progression-free survival; HR, hazard ratio; AUC, area under the curve; CI, confidence interval; NOX, NADPH oxidase; MYB, MYB proto-oncogene, transcription factor; GABARAPL2, GABA type A receptor associated protein like 2; HCAR1, hydroxycarboxylic acid receptor 1; TF, transferrin; AKR1C2, aldo-keto reductase family 1 member C2; DUOX1, dual oxidase 1; FXN, frataxin; RBMS1, RNA binding motif single stranded interacting protein 1.

most important risk factors. It had good performance in the evaluation of 6-9-year PFS; AUC of the 6-year PFS was >0.8 (Fig. 3D). The HR of the high-risk group was 2.827 (Fig. 2D).

Together, there were 14 unique key ferroptosis genes identified in STAD (the combination of the nine features in the OS model and the nine features in the PFS model), among which, NOX4, NOX5, AKR1C2, RBMS1, GABARAPL2, GJA1, TF and HCAR1 may be the most important carcinogenic genes (risk genes).

Roles of key genes in STAD. Among the 14 key genes in STAD, MYB, NOX4, PVT1 and PRR5 exhibited increased expression in STAD tumors compared with normal tissue (Fig. 4A). NOX4, AKR1C2, GJA1, GABARAPL2, HCAR1, RBMS1 and TF expression tended to increase from stages I to IV (Fig. 4B). TF, RBMS1, NOX5, NOX4, HCAR1, GJA1 and GABARAPL2 were significant risk factors for OS and PFS (Fig. 4C). Moreover, NOX5 was a significant risk factor not only for OS and PFS, but also for disease-free interval and DSS. The associations between key genes and important cancer pathways are shown in Fig. 4D. These genes suppress apoptosis and cell cycle progression but promote epithelial-mesenchymal transition (EMT) and activate protein kinase B and receptor tyrosine kinase (44-49).

Tumor immunity associated with key ferroptosis genes in STAD. The present study focused on key ferroptosis genes correlated (r>0.3; P<0.001) with immune cells in STAD tumors. GABARAPL2 and GJA1 expression was positively associated with macrophages (Fig. 5A and B). TF expression

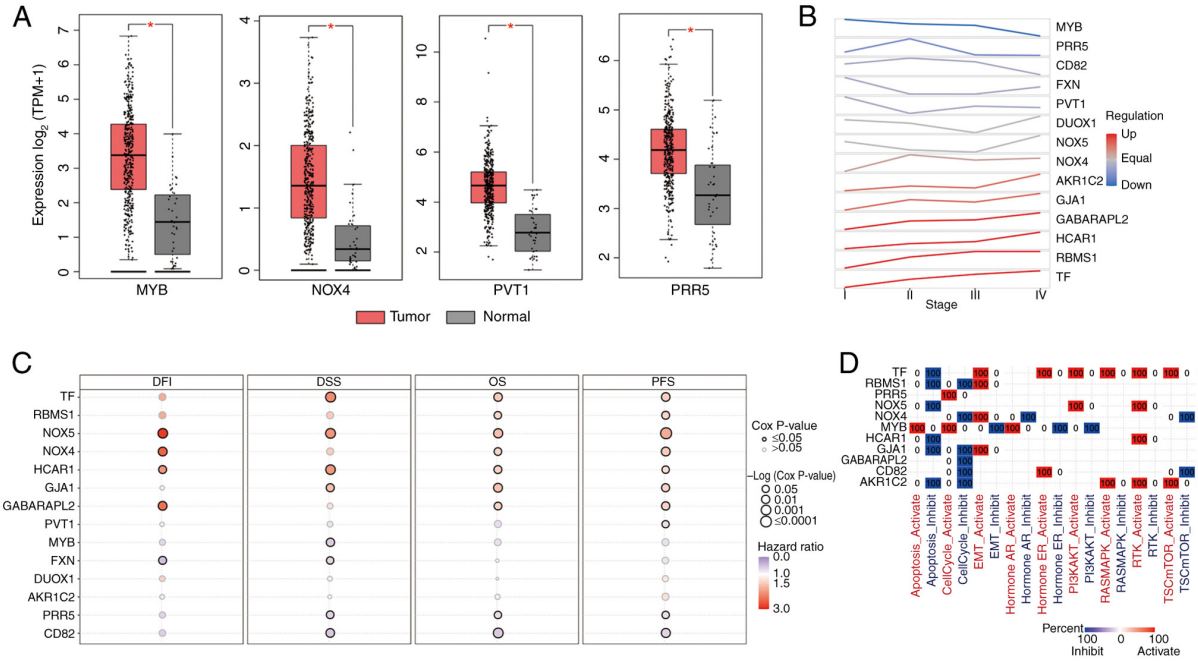

Figure 4. Roles of key ferroptosis genes in STAD. (A) Among the 14 key genes in STAD, MYB, NOX4, PVT1 and PRR5 expression was increased in STAD tumors compared with normal tissue. *P<0.05. (B) Expression trend of each key gene from stages I to IV. (C) Risk genes for DFI, DSS, OS and PFS among the 14 key genes. (D) Association between key genes and cancer pathways. STAD, stomach adenocarcinoma; DFI, disease-free interval; DSS, disease-specific survival; OS, overall survival; PFS, progression-free survival; NOX, NADPH oxidase; MYB, MYB proto-oncogene, transcription factor; PRR5, proline-rich protein 5; PVT1, Pvt1 oncogene; TF, transferrin; GABARAPL2, GABA type A receptor associated protein like 2; GJA1, gap junction protein α1; HCAR1, hydroxycarboxylic acid receptor 1; AKR1C2, aldo-keto reductase family 1 member C2; DUOX1, dual oxidase 1; FXN, frataxin; RBMS1, RNA binding motif single stranded interacting protein 1; TPM, transcripts per million; A, activation; I, inhibition.

was positively associated with $CD4^+$ T cells (Fig. 5C). The NOX4 expression levels were positively correlated with the levels of macrophages, neutrophils and dendritic cells (Fig. 5D). RBMS1 expression was positively correlated with $CD4^+$ T cells, macrophages and dendritic cells (Fig. 5E). These results suggest these key ferroptosis genes may impact the immune microenvironment.

Key gene interaction networks. Using the GeneMANIA online tool, GJA1, NOX4, NOX5 and TF hub genes were identified in a co-expression network of 14 key genes (Fig. 6A). RBMS1, GJA1, NOX5 and TF were key nodes in the genetic interaction network (Fig. 6B), while FXN and GABARAPL2 were important nodes in the physical interaction network (Fig. 6C).

Potential miRNAs that target key carcinogenic ferroptosis genes in STAD. Key genes were selected based on significant prognostic weights in the Cox model (absolute value of coefficients >0.05), positive correlation between gene expression and tumor staging, or significant association with poor survival in univariate analysis (P<0.05). As a result, seven genes were regarded as key carcinogenic ferroptosis genes in STAD among the 14 key ferroptosis genes. Using the miRWalk database, the miRNAs targeting these seven genes were downloaded. hsa-miR-505-5p and hsa-miR-6795-5p presented the most targets (12 and 11 targets, respectively; Fig. 7A). In addition, the top miRNAs with paired key genes (six genes each) were hsa-miR-6795-5p, hsa-miR-6758-5p, hsa-miR-501-5p and hsa-miR-484 (Fig. 7B). Therefore, these miRNAs (hsa-miR-6795-5p, hsa-miR-6758-5p, hsa-miR-501-5p, hsa-miR-505-5p and hsa-miR-484) may have potential therapeutic value for STAD; targets of these miRNAs are presented in Fig. 7C.

Through target gene prediction and pathway association analysis, target genes of miR-501-5P and miR-484 involved in core ferroptosis-related biological processes such as lipid peroxidation, iron ion metabolism and oxidative stress were identified (50-52). By contrast, the other candidates lacked direct literature support or had unknown functional relevance and require further investigation. miR-501-5p and miR-484 expression was evaluated in GC and surrounding normal tissue. miR-484 expression was decreased, while miR-501-5P expression was increased, in cancer tissues compared with normal tissue (Fig. 7E and G). miR-484 was overexpressed and miR-501-5p was knocked down in AGS cells (Fig. 7D and F). Overexpression of miR-484 and the knockdown of miR-501-5p significantly decreased the expression of the GC-associated high-risk genes AKR1C2, RBMS1, NOX4 and TF (Fig. 7H).

Potential drugs based on key ferroptosis genes in STAD. Using the GDSC and CTRP databases, potential drugs were identified on the basis of the seven key ferroptosis-related carcinogenic genes. The top 30 ranked drugs in the GDSC and CTRP databases are shown in Fig. 8A and B. The present study focused on drugs with multiple targets (which may have greater therapeutic value). In the CTRP database, four drugs had the most targets (targeting three genes): PHA-793887, SNS-032, CR-1-31B and saracatinib (Fig. 8C). According to the GDSC database (Fig. 8D), six drugs targeted four genes

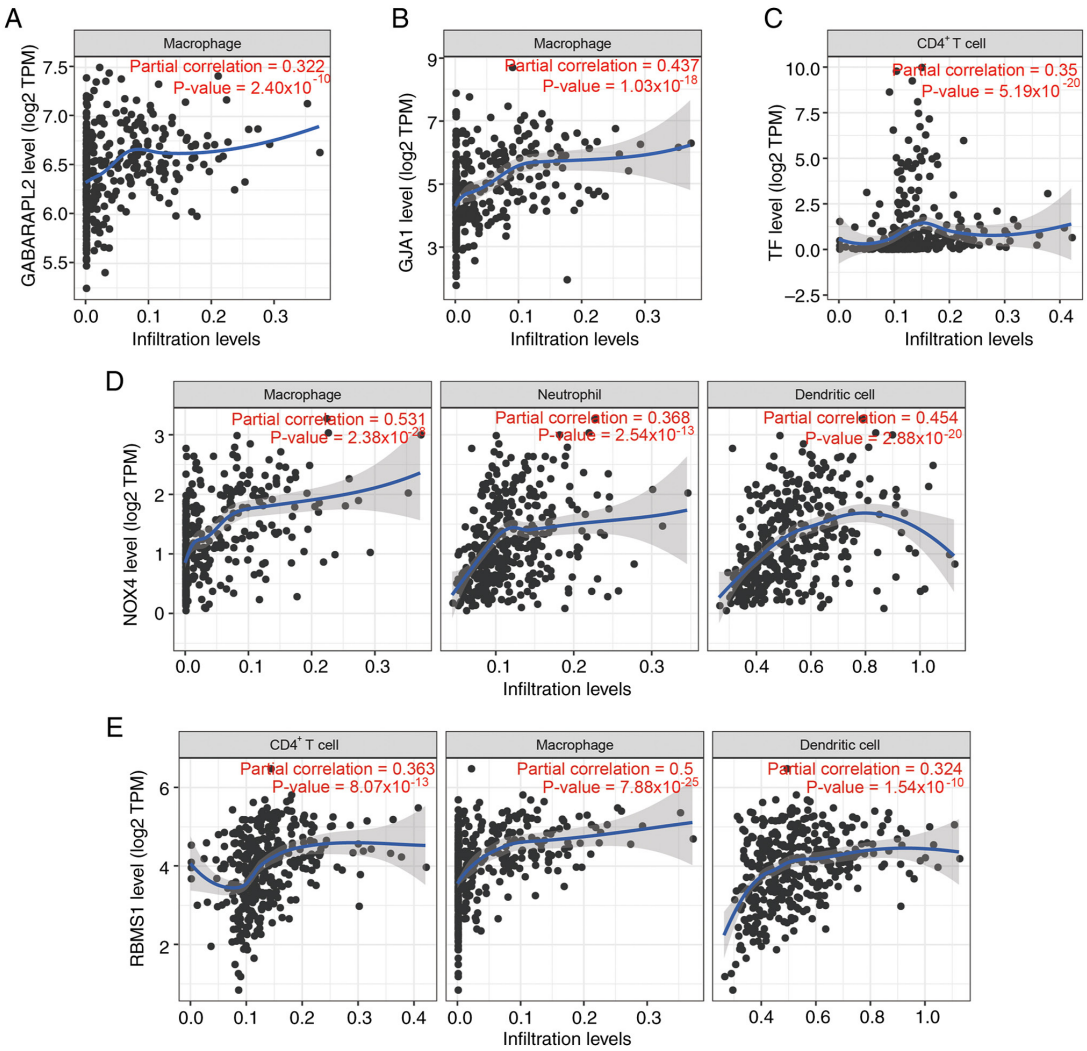

Figure 5. Tumor immunity association with key ferroptosis genes in stomach adenocarcinoma. (A) GABARAPL2 and (B) GJA1 expression is positively associated with macrophages. (C) TF is positively associated with CD4+ T cells. (D) NOX4 expression is positively correlated with macrophages, neutrophils and dendritic cells. (E) RBMS1 is positively correlated with CD4+ T cells, macrophages and dendritic cells. GABARAPL2, GABA type A receptor associated protein-like 2; GJA1, gap junction protein α1; TF, transferrin; NOX, NADPH oxidase; RBMS1, RNA-binding motif single stranded interacting protein 1; TPM, transcripts per million.

simultaneously: (5Z)-7-Oxozeaenol, selumetinib, RDEA119, AZ628, dabrafenib and trametinib. Together, these drugs may be candidate ferroptosis-related medications for the treatment of STAD. In AGS cells, all six drugs significantly induced GC cell death to varying degrees (Fig. 8E-J), and significantly reduced the expression of the high-risk genes (Fig. 8K).

Discussion

The present study investigated the key ferroptosis-associated genes involved in STAD development. A total of 14 key genes was identified, including seven carcinogenic genes that promote STAD development and are risk factors for survival. For OS and PFS prediction, two models were constructed; by combining age and stage information, another powerful OS model was generated. GABARAPL2, GJA1, NOX4 and RBMS1 may impact the immune microenvironment. Moreover, five miRNAs (hsa-miR-6795-5p, hsa-miR-6758-5p, hsa-miR-501-5p, hsa-miR-505-5p and hsa-miR-484) with potential therapeutic value for STAD were identified via the targeting of carcinogenic genes. Finally, it was hypothesized that the following drugs may be effective in treating STAD: (5Z)-7-Oxozeaenol, selumetinib, RDEA119, AZ628, dabrafenib and trametinib.

Unlike previous studies focusing on individual ferroptosis regulators (such as GPX4 or SLC7A11), the present work identified a novel seven-gene risk signature that predicts GC prognosis (53-55). This multi-gene approach provides a more comprehensive framework for targeting ferroptosis in heterogeneous tumors. The present results align with previous report linking ferroptosis resistance to GC metastasis but identified RBMS1 as a dual regulator of iron metabolism and EMT (44,56).

In the current optimized Cox hazard model, the log-rank P-value of OS was $2.55x10^{-14}$. To the best of our knowledge, this value is the lowest among all currently available models. Previous studies have established prognostic models with log-rank P-values (high- vs. low-risk) ranging from 0.0001 to 0.0100 (1,57-61). Moreover, the AUC of the ROC curve for the prediction of PFS was >0.8, which is markedly

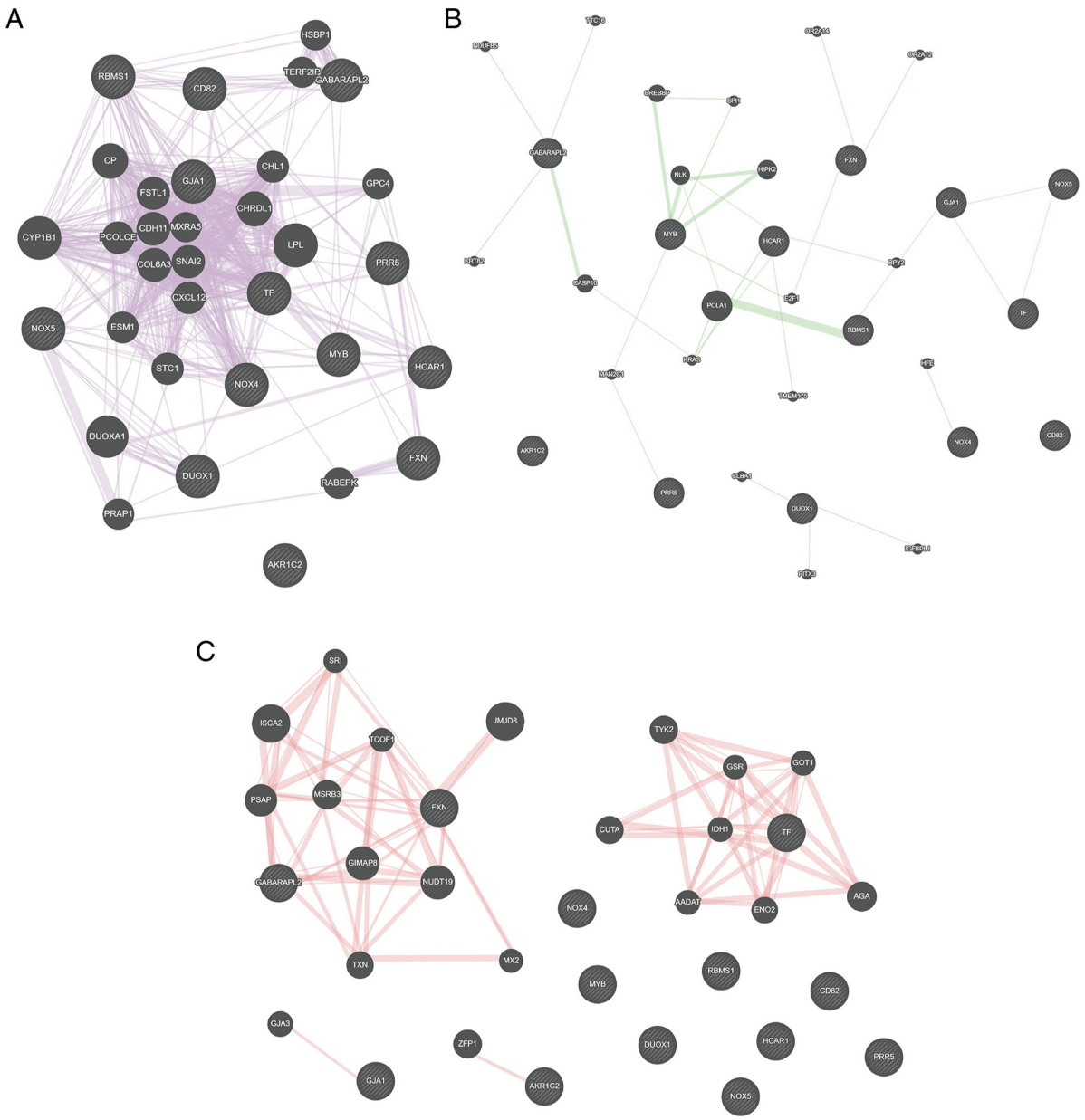

Figure 6. Key gene interaction networks. (A) Co-expression network. (B) Genetic interaction network. (C) Physical interaction network.

improved compared with that reported in the majority of previous studies (1,61,62). A previous study explored novel immune ferroptosis-related genes associated with clinical and prognostic features in patients with GC (38). However, performance of the model was not satisfactory (P=0.046 in the test cohort; the best AUC value was ~0.7). In summary, the present prognostic model constructed using ferroptosis genes is one of the best performing models for GC prognosis.

On the basis of the coefficients of the prognostic model, the interaction networks and association with tumor immunity, it was found that NOX5, NOX4 and GABARAPL2 served more prominent cancer-promoting roles compared with the other key genes. NOX5 is a strong reactive oxygen species producer. It mediates the crosstalk between tumor cells and cancer-associated fibroblasts by regulating the cytokine network (63). To the best of our knowledge, only one study has investigated the genetic alteration and mRNA expression of the NOX family in patients with GC (63), the aforementioned bioinformatics study demonstrated decreased NOX5 expression in GC; to the best of our knowledge, however, no study has elucidated the role of NOX5 in GC. The present study highlights the prognostic and carcinogenic role of NOX5 in GC and hence expands the range of GC targets. As shown in a previous study (46), NOX4 expression was also increased in GC compared with normal tissues, which is in line with the present findings. Additionally, the aforementioned study reported NOX4 is a potential prognostic marker in GC and implicate that the use of NOX inhibitor targeting NOX4 and DUOX1 may be an effective strategy for GC therapy (46). NOX4 was a valid biomarker for STAD (64). Similarly, a previous study involving LASSO analysis used NOX4 for the construction of a hypoxia-related gene prognostic model for GC (65). However, none of the aforementioned studies revealed the cancer-promoting mechanism of NOX4. By contrast, the present study suggested that NOX4

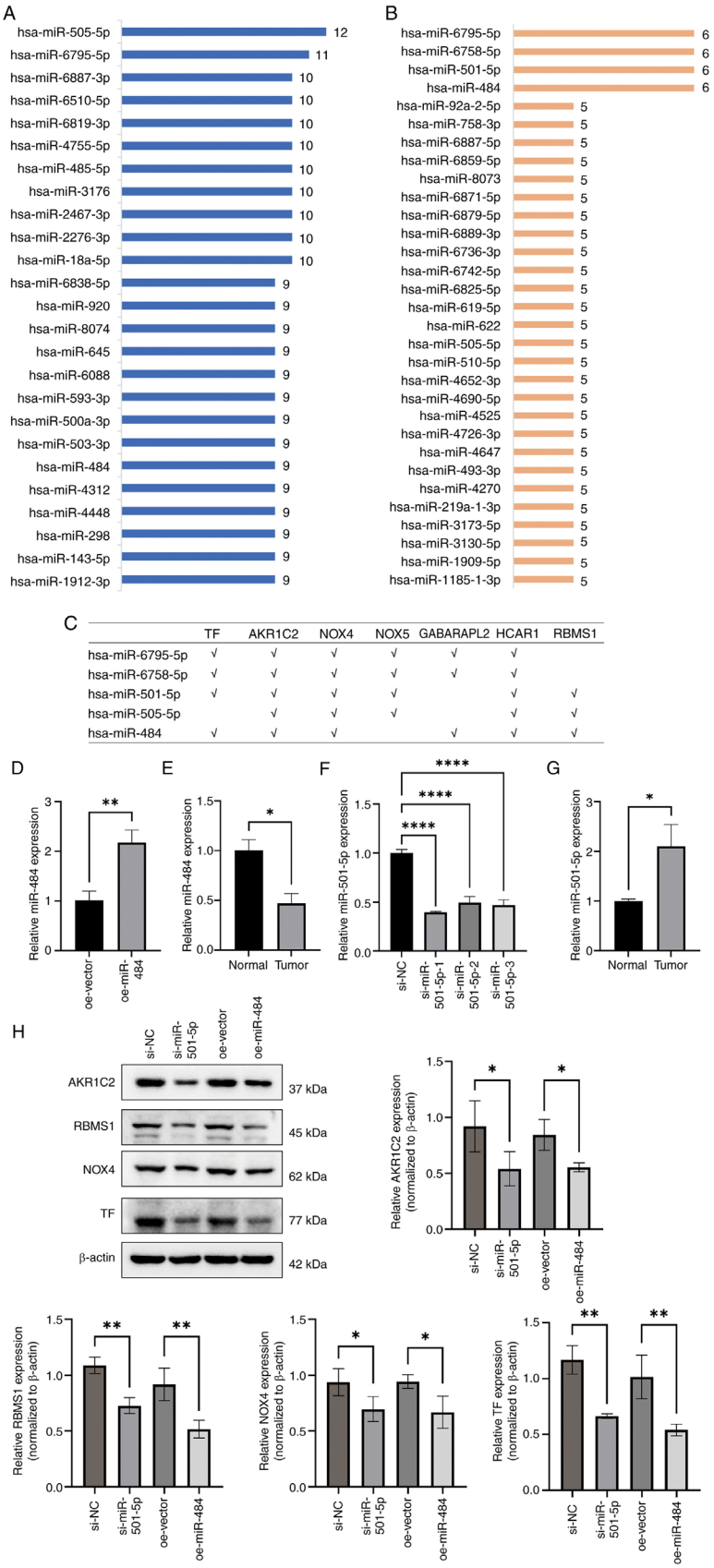

Figure 7. Potential miRNAs that target key carcinogenic ferroptosis genes in stomach adenocarcinoma. (A) Top miRNAs with the most matching pairs to key genes. (B) Top miRNAs with the most targeted genes. (C) A total of five miRNAs (hsa-miR-6795-5p, hsa-miR-6758-5p, hsa-miR-501-5p, hsa-miR-505-5p and hsa-miR-484) targeted the majority of genes (six targets each). Relative mRNA expression of miR-484 in (D) GC cells with miR-484 overexpression and (E) tumor and surrounding normal tissue. Relative mRNA expression of miR-501-5p in (F) GC cell line treated with siRNAs and (G) tumor and surrounding normal tissue. (H) A total of four risk genes for GC (AKR1C2, RBMS1, NADPH oxidase 4 and TF) were detected via western blotting. *P<0.05; **P<0.01; ****P<0.001. miRNA/miR, microRNA; hsa, *Homo sapiens*; GC, gastric cancer; siRNA, small interfering RNA; nc, negative control; oe, overexpression; GABARAPL2, GABA type A receptor-associated protein-like 2; TF, transferrin; AKR1C2, aldo-keto reductase family 1 member C2; NOX, NADPH oxidase; HCAR1, hydroxycarboxylic acid receptor 1; RBMS1, RNA binding motif single stranded interacting protein 1.

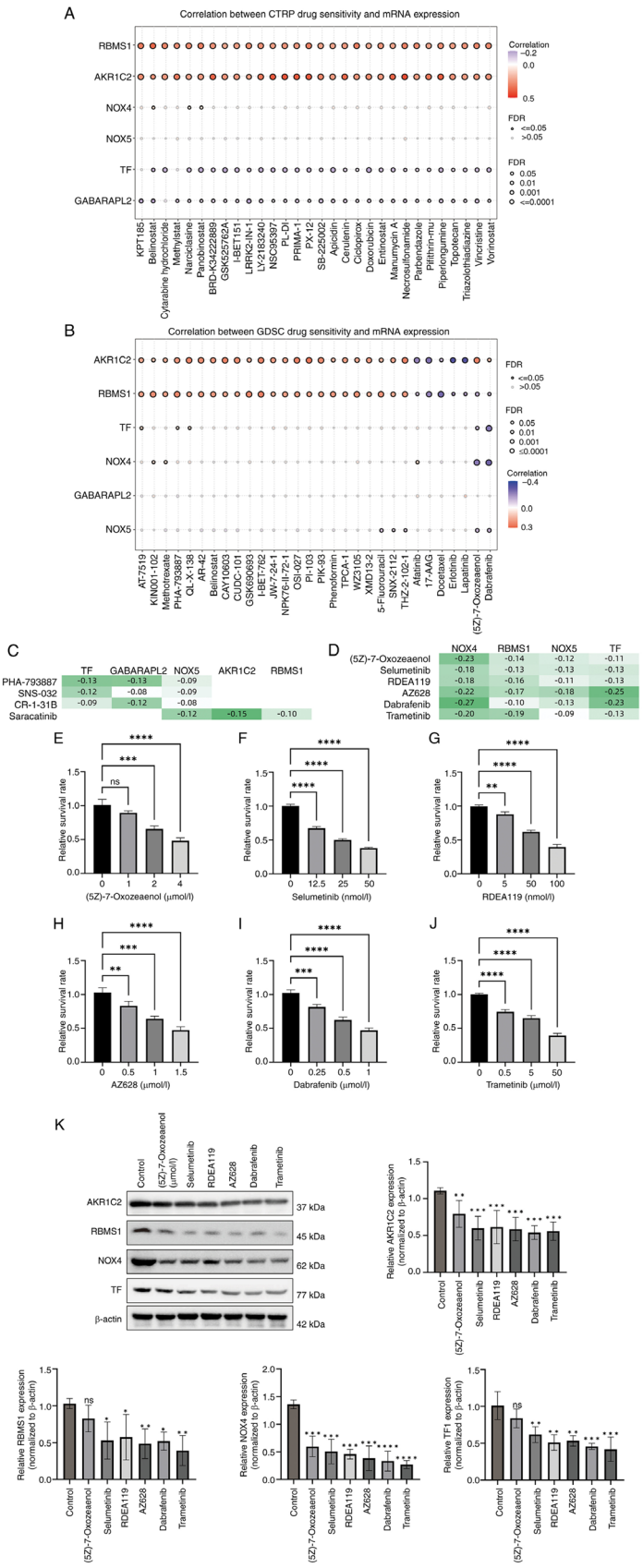

Figure 8. Potential drugs based on key ferroptosis genes in stomach adenocarcinoma. Top 30 ranked drugs in (A) GDSC and (B) CTRP database based on the seven key carcinogenic genes. (C) In the CTRP database, the following four drugs had the most targets (each targeting three genes): PHA-793887, SNS-032, CR-1-31B and saracatinib. (D) In the GDSC database, six drugs targeted four genes simultaneously, namely (5Z)-7-oxozeaenol, selumetinib, RDEA119, AZ628, dabrafenib and trametinib. Drug toxicity of (E) (5Z)-7-oxozeaenol, (F) selumetinib, (G) RDEA119, (H) AZ628, (I) dabrafenib and (J) trametinib towards gastric cancer cells. (K) Expression of four risk genes (AKR1C2, RBMS1, NOX4 and TF) was downregulated in gastric cancer cells treated with the aforementioned drugs. *P<0.05; **P<0.01; ***P<0.005; ****P<0.001. GDSC, Genomics of Drug Sensitivity in Cancer; CTRP, Cancer Therapeutics Response Portal; AKR1C2, aldo-keto reductase family 1 member C2; RBMS1, RNA-binding motif single stranded interacting protein 1; NOX, NADPH oxidase; TF, transferrin; FDR, false discovery rate; ns, not significant.

and NOX5 (two important ferroptosis drivers) may drive GC progression by promoting ferroptosis.

GABARAPL2 is a mitophagy-related gene (66-69) and a ferroptosis driver. A previous study established and validated a nomogram model based on GABARAPL2 and cell division cycle 37, HSP90 cochaperone (CDC37) (49). GABARAPL2 and CDC37 display different immune infiltration states and are prognostic biomarkers and candidate therapeutic targets of GC (49). Another study revealed different expression patterns of GABARAPL2 in GC and normal tissues, but it was not a powerful independent prognostic factor (70). The present study revealed that ferroptosis drivers, but not inhibitors, serve primarily pro-carcinogenic roles, suggesting that the inhibition of ferroptosis is a potential strategy to combat GC progression.

The present study identified miRNAs (hsa-miR-6795-5p, hsa-miR-6758-5p, hsa-miR-501-5p, hsa-miR-505-5p and hsa-miR-484) with potential therapeutic implications. A previous study revealed that the upregulation of miR-501-5p activates the Wnt/β-catenin signaling pathway and enhances the stem cell-like phenotype in GC (71), and another study revealed that miRNA-501-5p promotes cell proliferation and migration in GC by downregulating lysophosphatidic acid receptor 1 (72). The aforementioned conclusions contradict that of the present study; thus, whether hsa-miR-501-5p exerts an anticancer effect remains to be determined. The expression of miR-484 is downregulated in GC (73). In 2020, an *in vitro* study revealed that miR-484 suppresses the proliferation, migration and invasion, and induces the apoptosis of GC cells (74). Moreover, downregulation of miR-484 is associated with poor prognosis and GC progression (75). The aforementioned studies are consistent with the present hypothesis that miR-484 may serve as a potential molecular agent against GC progression. The present study experimentally validated miR-484 and miR-501-5p due to their established roles in ferroptosis-associated processes. miR-484 was downregulated in GC tissues. Through its seed sequence 5'-UCAGG-3', miR-484 targets the 3'-UTRs of NOX4, TF, and RBMS1, inducing mRNA degradation and reducing target protein expression by 60-70%. Consequently, it blocks NADPH oxidase activity, iron ion uptake, and reverses epithelial-mesenchymal transition, synergistically inhibiting ferroptosis, immune evasion, and metastasis (44,76). Regarding miR-501-5p, experimental inhibition of this miRNA unexpectedly reduced the expression of target genes AKR1C2 and GABARAPL2. This paradoxical effect may stem from: (1) indirect regulatory networks (e.g., miR-501-5p suppresses tumor suppressors LPAR1; inhibiting miR-501-5p elevates LPAR1 expression, indirectly reducing AKR1C2) (72); (2) ceRNA competitive mechanisms (77); and (3) miRNA concentration-dependent effects. These findings reveal its dual role in directly targeting oncogenes while indirectly maintaining oncogenic networks. The other miRNAs (miR-6795-5p, miR-6758-5p and hsa-miR-505-5p) represent novel candidates with potential therapeutic value but require functional characterization in future.

A panel of drugs (5Z-7-oxozeaenol, selumetinib, RDEA119, AZ628, dabrafenib and trametinib) for the treatment of STAD was investigated in the present study. 5Z-7-oxozeaenol is a selective TGFβ-activated kinase 1 inhibitor (78). A previous study reported that 5Z-7-oxozeaenol increases the expression levels of cytosolic cytochrome *c* and cleaved caspase 3 and apoptosis rate in GC cells (79). Despite the different mechanisms, the results are consistent with the conclusions of the present study, and support the potential of 5Z-7-oxozeaenol as a candidate anti-GC drug. The MEK inhibitor selumetinib is a potent, orally active inhibitor of the MAPK/ERK pathway, and *in vitro* experiments suggested that selumetinib should be validated in prospective clinical trials (80). Moreover, the VIKTORY trial was designed to classify patients with metastatic GC on the basis of clinical sequencing and focused on eight biomarker groups, among which, selumetinib was evaluated with or without chemotherapy (81). However, the effectiveness of selumetinib in the clinic is not yet clear. Similar to selumetinib, RDEA119 is a MEK inhibitor that exhibits an anticancer effect on multiple cancer cells, including GC cells (82). The potential for improving tumor microenvironment of AZ628 has been proposed in another bioinformatics study, but no validation was performed (83). Dabrafenib is a BRAF inhibitor and its action on GC may increase susceptibility to immunotherapy (84). Recently, the US Food and Drug Administration accelerated the approval of darafenib in combination with trametinib for the treatment of unresectable or metastatic solid tumors (including GC) with the BRAFV600E mutation, and this combination has been recommended in the latest National Comprehensive Cancer Network guidelines for GC (85). Trametinib is a MEK inhibitor used to inhibit the growth of GC (86-88). In addition, the combination of dabrafenib and trametinib may be promising in the clinical treatment of GC.

The present study has limitations. Regarding bioinformatics methods, LASSO regression performance is greatly influenced by data quality. The present study uses three databases, and the sample size was limited. In the future, it is necessary to expand the database samples and optimize the data quality to obtain more accurate results. LASSO regression selects the most important variables, but the explanatory power of these variables may be low. Therefore, it may be necessary to combine other analytical methods to improve the explanatory power of LASSO regression in the future. Although numerous key genes, miRNAs and inhibitors have been screened, the interaction between them and the regulatory mechanism of iron-mediated cell death remains unclear. The present results should be verified through basic experiments and clinical research. While weighted correlation network analysis and LASSO regression robustly identify gene signatures, these approaches may overlook non-linear gene interactions. Additionally, bulk RNA-sequencing data cannot resolve cell type-specific ferroptosis mechanisms, necessitating future single-cell analyses. Prioritized targets (such as NOX4) should be validated using NOX4-knockout AGS cell lines and patient-derived xenograft models treated with ferroptosis inducers erastin/artesunate, alongside RNA interference-mediated gene silencing.

In summary, 14 key ferroptosis-related genes, including seven carcinogenic genes, that promoted STAD development and are risk factors for survival were identified in the present study. For OS and PFS prediction, two models were constructed, and five miRNAs (hsa-miR-6795-5p, hsa-miR-6758-5p, hsa-miR-501-5p, hsa-miR-505-5p and hsa-miR-484) with potential therapeutic value for STAD were identified through the targeting of carcinogenic genes. The present results revealed that

(5Z)-7-oxozeaenol, selumetinib, RDEA119, AZ628, dabrafenib and trametinib may be effective in treating STAD.

Acknowledgements

Not applicable.

Funding

The present study was supported by Kunming Medical University First Affiliated Hospital Science and Technology Talent Training Program (Leading Talent; grant no. L-2019024), Sub-project of Yunnan Clinical Medical Research Center (grant no. 202102AA100062), Scientific Research Fund Project of Yunnan Education Department (grant no. 2024Y223), Kunming Medical University graduate Student Innovation Fund (grant no. 2024S045), Yunnan Fundamental Research Projects (grant no. 202401AT070170) and First-Class Discipline Team of Kunming Medical University (grant no. 2024XKTDYS02).

Availability of data and materials

The data generated in the present study may be requested from the corresponding author.

Authors' contributions

HW conceived and designed the study, analyzed data and wrote the manuscript. HC conceived and designed the study, interpreted data and edited the manuscript. JJL and DZ performed experiments and analyzed data. DW analyzed data. MSH and MWL interpreted data and constructed figures. SYH interpreted data. LQM conceived and designed the study. HW and LQM confirm the authenticity of all the raw data. All authors read and approved the final manuscript.

Ethics approval and consent to participate

Ethics approval was obtained from the ethics committee of the First Affiliated Hospital of Kunming Medical University (approval no. 2024 lunshen L No.78). The procedures used in the present study adhere to the principles of CFDA/GCP and the Declaration of Helsinki. All participants provided voluntary written informed consent.

Patient consent for publication

Not applicable.

Competing interests

The authors declare that they have no competing interests.

References

1. Chang J, Wu H, Wu J, Liu M, Zhang W, Hu Y, Zhang X, Xu J, Li L, Yu P and Zhu J: Constructing a novel mitochondrial-related gene signature for evaluating the tumor immune microenvironment and predicting survival in stomach adenocarcinoma. J Transl Med 21: 191, 2023.
2. Jin W, Ou K, Li Y, Liu W and Zhao M: Metabolism-related long noncoding RNA in the stomach cancer associated with 11 AMMLs predictive nomograms for OS in STAD. Front Genet 14: 1127132, 2023.
3. Wang J, Liu D, Wang Q and Xie Y: Identification of basement membrane-related signatures in gastric cancer. Diagnostics (Basel) 13: 1844, 2023.
4. Wu B, Fu L, Guo X, Hu H, Li Y, Shi Y, Zhang Y, Han S, Lv C and Tian Y: Multiomics profiling and digital image analysis reveal the potential prognostic and immunotherapeutic properties of CD93 in stomach adenocarcinoma. Front Immunol 14: 984816, 2023.
5. Zhao W, Lin J, Cheng S, Li H, Shu Y and Xu C: Comprehensive analysis of COMMD10 as a novel prognostic biomarker for gastric cancer. PeerJ 11: e14645, 2023.
6. Zhao Z, Mak TK, Shi Y, Li K, Huo M and Zhang C: Integrative analysis of cancer-associated fibroblast signature in gastric cancer. Heliyon 9: e19217, 2023.
7. Sung H, Ferlay J, Siegel RL, Laversanne M, Soerjomataram I, Jemal A and Bray F: Global cancer statistics 2020: GLOBOCAN estimates of incidence and mortality worldwide for 36 cancers in 185 countries. CA Cancer J Clin 71: 209-249, 2021.
8. Ajani JA, Lee J, Sano T, Janjigian YY, Fan D and Song S: Gastric adenocarcinoma. Nat Rev Dis Primers 3: 17036, 2017.
9. Takahari D: Second-line chemotherapy for patients with advanced gastric cancer. Gastric Cancer 20: 395-406, 2017.
10. Johnston FM and Beckman M: Updates on management of gastric cancer. Curr Oncol Rep 21: 67, 2019.
11. Hirschhorn T and Stockwell BR: The development of the concept of ferroptosis. Free Radic Biol Med 133: 130-143, 2019.
12. Gao W, Wang X, Zhou Y, Wang X and Yu Y: Autophagy, ferroptosis, pyroptosis, and necroptosis in tumor immunotherapy. Signal Transduct Target Ther 7: 196, 2022.
13. Liang D, Minikes AM and Jiang X: Ferroptosis at the intersection of lipid metabolism and cellular signaling. Mol Cell 82: 2215-2227, 2022.
14. Liu J, Kang R and Tang D: Signaling pathways and defense mechanisms of ferroptosis. FEBS J 289: 7038-7050, 2022.
15. Liu P, Wang W, Li Z, Li Y, Yu X, Tu J and Zhang Z: Ferroptosis: A new regulatory mechanism in osteoporosis. Oxid Med Cell Longev 2022: 2634431, 2022.
16. Yang Y, Wang Y, Guo L, Gao W, Tang TL and Yan M: Interaction between macrophages and ferroptosis. Cell Death Dis 13: 355, 2022.
17. Zhao L, Zhou X, Xie F, Zhang L, Yan H, Huang J, Zhang C, Zhou F, Chen J and Zhang L: Ferroptosis in cancer and cancer immunotherapy. Cancer Commun (Lond) 42: 88-116, 2022.
18. Gong C, Ji Q, Wu M, Tu Z, Lei K, Luo M, Liu J, Lin L, Li K, Li J, *et al*: Ferroptosis in tumor immunity and therapy. J Cell Mol Med 26: 5565-5579, 2022.
19. Li J, Liu J, Xu Y, Wu R, Chen X, Song X, Zeh H, Kang R, Klionsky DJ, Wang X and Tang D: Tumor heterogeneity in autophagy-dependent ferroptosis. Autophagy 17: 3361-3374, 2021.
20. Liao P, Wang W, Wang W, Kryczek I, Li X, Bian Y, Sell A, Wei S, Grove S, Johnson JK, *et al*: CD8(+) T cells and fatty acids orchestrate tumor ferroptosis and immunity via ACSL4. Cancer Cell 40: 365-378.e6, 2022.
21. Luo T, Wang Y and Wang J: Ferroptosis assassinates tumor. J Nanobiotechnology 20: 467, 2022.
22. Fu D, Wang C, Yu L and Yu R: Induction of ferroptosis by ATF3 elevation alleviates cisplatin resistance in gastric cancer by restraining Nrf2/Keap1/xCT signaling. Cell Mol Biol Lett 26: 26, 2021.
23. Gu R, Xia Y, Li P, Zou D, Lu K, Ren L, Zhang H and Sun Z: Ferroptosis and its Role in Gastric Cancer. Front Cell Dev Biol 10: 860344, 2022.
24. Huang G, Xiang Z, Wu H, He Q, Dou R, Lin Z, Yang C, Huang S, Song J, Di Z, *et al*: The lncRNA BDNF-AS/WDR5/FBXW7 axis mediates ferroptosis in gastric cancer peritoneal metastasis by regulating VDAC3 ubiquitination. Int J Biol Sci 18: 1415-1433, 2022.
25. Li D, Wang Y, Dong C, Chen T, Dong A, Ren J, Li W, Shu G, Yang J, Shen W, *et al*: CST1 inhibits ferroptosis and promotes gastric cancer metastasis by regulating GPX4 protein stability via OTUB1. Oncogene 42: 83-98, 2023.
26. Lin Z, Song J, Gao Y, Huang S, Dou R, Zhong P, Huang G, Han L, Zheng J, Zhang X, *et al*: Hypoxia-induced HIF-1α/lncRNA-PMAN inhibits ferroptosis by promoting the cytoplasmic translocation of ELAVL1 in peritoneal dissemination from gastric cancer. Redox Biol 52: 102312, 2022.

27. Liu Y, Song Z, Liu Y, Ma X, Wang W, Ke Y, Xu Y, Yu D and Liu H: Identification of ferroptosis as a novel mechanism for anti-tumor activity of natural product derivative a2 in gastric cancer. Acta Pharm Sin B 11: 1513-1525, 2021.
28. Ma M, Kong P, Huang Y, Wang J, Liu X, Hu Y, Chen X, Du C and Yang H: Activation of MAT2A-ACSL3 pathway protects cells from ferroptosis in gastric cancer. Free Radic Biol Med 181: 288-299, 2022.
29. Ouyang S, Li H, Lou L, Huang Q, Zhang Z, Mo J, Li M, Lu J, Zhu K, Chu Y, *et al*: Inhibition of STAT3-ferroptosis negative regulatory axis suppresses tumor growth and alleviates chemoresistance in gastric cancer. Redox Biol 52: 102317, 2022.
30. Song S, Wen F, Gu S, Gu P, Huang W, Ruan S, Chen X, Zhou J, Li Y, Liu J and Shu P: Network pharmacology study and experimental validation of Yiqi Huayu decoction inducing ferroptosis in gastric cancer. Front Oncol 12: 820059, 2022.
31. Wang Y, Zheng L, Shang W, Yang Z, Li T, Liu F, Shao W, Lv L, Chai L, Qu L, *et al*: Wnt/beta-catenin signaling confers ferroptosis resistance by targeting GPX4 in gastric cancer. Cell Death Differ 29: 2190-2202, 2022.
32. Xu C, Liu Z and Xiao J: Ferroptosis: A double-edged sword in gastrointestinal disease. Int J Mol Sci 22: 12403, 2021.
33. Xu X, Li Y, Wu Y, Wang M, Lu Y, Fang Z, Wang H and Li Y: Increased ATF2 expression predicts poor prognosis and inhibits sorafenib-induced ferroptosis in gastric cancer. Redox Biol 59: 102564, 2023.
34. Yang H, Hu Y, Weng M, Liu X, Wan P, Hu Y, Ma M, Zhang Y, Xia H and Lv K: Hypoxia inducible lncRNA-CBSLR modulates ferroptosis through m6A-YTHDF2-dependent modulation of CBS in gastric cancer. J Adv Res 37: 91-106, 2022.
35. Yang Z, Zou S, Zhang Y, Zhang J, Zhang P, Xiao L, Xie Y, Meng M, Feng J, Kang L, *et al*: ACTL6A protects gastric cancer cells against ferroptosis through induction of glutathione synthesis. Nat Commun 14: 4193, 2023.
36. Zhang H, Wang M, He Y, Deng T, Liu R, Wang W, Zhu K, Bai M, Ning T, Yang H, *et al*: Chemotoxicity-induced exosomal lncFERO regulates ferroptosis and stemness in gastric cancer stem cells. Cell Death Dis 12: 1116, 2021.
37. Lee JY, Nam M, Son HY, Hyun K, Jang SY, Kim JW, Kim MW, Jung Y, Jang E, Yoon SJ, *et al*: Polyunsaturated fatty acid biosynthesis pathway determines ferroptosis sensitivity in gastric cancer. Proc Natl Acad Sci USA 117: 32433-32442, 2020.
38. Xiao C, Dong T, Yang L, Jin L, Lin W, Zhang F, Han Y and Huang Z: Identification of novel immune ferropotosis-related genes associated with clinical and prognostic features in gastric cancer. Front Oncol 12: 904304, 2022.
39. Deng H, Lin Y, Gan F, Li B, Mou Z, Qin X, He X and Meng Y: Prognostic model and immune infiltration of ferroptosis subcluster-related modular genes in gastric cancer. J Oncol 2022: 5813522, 2022.
40. Cheng X, Dai E, Wu J, Flores NM, Chu Y, Wang R, Dang M, Xu Z, Han G, Liu Y, *et al*: Atlas of metastatic gastric cancer links ferroptosis to disease progression and immunotherapy response. Gastroenterology 167: 1345-1357, 2024.
41. Yue Z, Yuan Y, Zhou Q, Sheng J and Xin L: Ferroptosis and its current progress in gastric cancer. Front Cell Dev Biol 12: 1289335, 2024.
42. Cancer Genome Atlas Research Network; Weinstein JN, Collisson EA, Mills GB, Shaw KR, Ozenberger BA, Ellrott K, Shmulevich I, Sander C and Stuart JM: The cancer genome atlas pan-cancer analysis project. Nat Genet 45: 1113-1120, 2013.
43. Livak KJ and Schmittgen TD: Analysis of relative gene expression data using real-time quantitative PCR and the 2(-Delta Delta C(T)) method. Methods 25: 402-408, 2001.
44. Liu M, Li H, Zhang H, Zhou H, Jiao T, Feng M, Na F, Sun M, Zhao M, Xue L and Xu L: RBMS1 promotes gastric cancer metastasis through autocrine IL-6/JAK2/STAT3 signaling. Cell Death Dis 13: 287, 2022.
45. Lodhi MS, Khan MT, Bukhari SMH, Sabir SH, Samra ZQ, Butt H and Akram MS: Probing transferrin receptor overexpression in gastric cancer mice models. ACS Omega 6: 29893-29904, 2021.
46. You X, Ma M, Hou G, Hu Y and Shi X: Gene expression and prognosis of NOX family members in gastric cancer. Onco Targets Ther 11: 3065-3074, 2018.
47. Zhang H, Zhan J, Zhou J, Liu L, He Y, Le Y, Liu W, Zhou L, Liu Y and Xiang X: Identification of HCAR1 as a ferroptosis-related biomarker of gastric cancer based on a novel ferroptosis-related prognostic model and in vitro experiments. Carcinogenesis 7: bgaf030, 2025.
48. Pourjamal N, Shirkoohi R, Rohani E and Hashemi M: The expression analysis of MEST1 and GJA1 genes in gastric cancer in association with clinicopathological characteristics. Int J Hematol Oncol Stem Cell Res 18: 83-91, 2024.
49. Wang Z, Chen C, Ai J, Shu J, Ding Y, Wang W, Gao Y, Jia Y and Qin Y: Identifying mitophagy-related genes as prognostic biomarkers and therapeutic targets of gastric carcinoma by integrated analysis of single-cell and bulk-RNA sequencing data. Comput Biol Med 163: 107227, 2023.
50. Huang DH, Wang GY, Zhang JW, Li Y, Zeng XC and Jiang N: MiR-501-5p regulates CYLD expression and promotes cell proliferation in human hepatocellular carcinoma. Jpn J Clin Oncol 45: 738-744, 2015.
51. Gu Y, Wu S, Fan J, Meng Z, Gao G, Liu T, Wang Q, Xia H, Wang X and Wu K: CYLD regulates cell ferroptosis through Hippo/YAP signaling in prostate cancer progression. Cell Death Dis 15: 79, 2024.
52. Huang M, Cheng S, Li Z, Chen J, Wang C, Li J and Zheng H: Preconditioning exercise inhibits neuron ferroptosis and ameliorates brain ischemia damage by skeletal muscle-derived exosomes via regulating miR-484/ACSL4 axis. Antioxid Redox Signal 41: 769-792, 2024.
53. Zhang J, Tian T, Li X, Yan Y, Zhao D, Ji S, Ni J, Zhang J, Liu K, Qing H and Quan Z: p53 inhibits OTUD5 transcription to promote GPX4 degradation and induce ferroptosis in gastric cancer. Clin Transl Med 15: e70271, 2025.
54. Lu D, Yuan L, Wang Z, Xu D, Meng F, Jia S, Li Y, Li W and Nan Y: Dioscin induces ferroptosis to suppress the metastasis of gastric cancer through the SLC7A11/GPX4 axis. Free Radic Res 59: 426-441, 2025.
55. Wang H, Li C, Meng S and Kuang YT: The LINC01094/miR-545-3p/SLC7A11 signaling axis promotes the development of gastric cancer by regulating cell growth and ferroptosis. Biochem Genet: https://doi.org/10.1007/s10528-024-10959-3.
56. Xu Y, Hao J, Chen Q, Qin Y, Qin H, Ren S, Sun C, Zhu Y, Shao B, Zhang J and Wang H: Inhibition of the RBMS1/PRNP axis improves ferroptosis resistance-mediated oxaliplatin chemoresistance in colorectal cancer. Mol Carcinog 63: 224-237, 2024.
57. Yu R, Li Z, Zhang C, Song H, Deng M, Sun L, Xu L, Che X, Hu X, Qu X, *et al*: Elevated limb-bud and heart development (LBH) expression indicates poor prognosis and promotes gastric cancer cell proliferation and invasion by upregulating Integrin/FAK/Akt pathway. PeerJ 7: e6885, 2019.
58. Berthelet E, Pickles T, Lee KW, Liu M and Truong PT; Prostate Cancer Outcomes Initiative: Long-term androgen deprivation therapy improves survival in prostate cancer patients presenting with prostate-specific antigen levels >20 ng/ml. Int J Radiat Oncol Biol Phys 63: 781-787, 2005.
59. Huang R, Lu TL and Zhou R: Identification and immune landscape analysis of fatty acid metabolism genes related subtypes of gastric cancer. Sci Rep 13: 20443, 2023.
60. Yuan Q, Deng D, Pan C, Ren J, Wei T, Wu Z, Zhang B, Li S, Yin P and Shang D: Integration of transcriptomics, proteomics, and metabolomics data to reveal HER2-associated metabolic heterogeneity in gastric cancer with response to immunotherapy and neoadjuvant chemotherapy. Front Immunol 13: 951137, 2022.
61. Wang X, Zhang W, Guo Y, Zhang Y, Bai X and Xie Y: Identification of critical prognosis signature associated with lymph node metastasis of stomach adenocarcinomas. World J Surg Oncol 21: 61, 2023.
62. Feng A, He L, Chen T and Xu M: A novel cuproptosis-related lncRNA nomogram to improve the prognosis prediction of gastric cancer. Front Oncol 12: 957966, 2022.
63. Chen J, Wang Y, Zhang W, Zhao D, Zhang L, Zhang J, Fan J and Zhan Q: NOX5 mediates the crosstalk between tumor cells and cancer-associated fibroblasts by regulating cytokine network. Clin Transl Med 11: e472, 2021.
64. Xiao R, Wang S, Guo J, Liu S, Ding A, Wang G, Li W, Zhang Y, Bian X, Zhao S and Qiu W: Ferroptosis-related gene NOX4, CHAC1 and HIF1A are valid biomarkers for stomach adenocarcinoma. J Cell Mol Med 26: 1183-1193, 2022.
65. Guo J, Xing W, Liu W, Liu J, Zhang J and Pang Z: Prognostic value and risk model construction of hypoxic stress-related features in predicting gastric cancer. Am J Transl Res 14: 8599-8610, 2022.
66. Chan JCY and Gorski SM: Unlocking the gate to GABARAPL2. Biol Futur 73: 157-169, 2022.
67. Polletta L, Vernucci E, Carnevale I, Arcangeli T, Rotili D, Palmerio S, Steegborn C, Nowak T, Schutkowski M, Pellegrini L, *et al*: SIRT5 regulation of ammonia-induced autophagy and mitophagy. Autophagy 11: 253-270, 2015.

68. Scicluna K, Dewson G, Czabotar PE and Birkinshaw RW: A new crystal form of GABARAPL2. Acta Crystallogr F Struct Biol Commun 77: 140-147, 2021.
69. Zhang Z, Gu H, Li Q, Zheng J, Cao S, Weng C and Jia H: GABARAPL2 is critical for growth restriction of *Toxoplasma gondii* in HeLa cells treated with gamma interferon. Infect Immun 88: e00054-e00020, 2020.
70. Wang M, Jing J, Li H, Liu J, Yuan Y and Sun L: The expression characteristics and prognostic roles of autophagy-related genes in gastric cancer. PeerJ 9: e10814, 2021.
71. Fan D, Ren B, Yang X, Liu J and Zhang Z: Upregulation of miR-501-5p activates the wnt/β-catenin signaling pathway and enhances stem cell-like phenotype in gastric cancer. J Exp Clin Cancer Res 35: 177, 2016.
72. Ma X, Feng J, Lu M, Tang W, Han J, Luo X, Zhao Q and Yang L: microRNA-501-5p promotes cell proliferation and migration in gastric cancer by downregulating LPAR1. J Cell Biochem 121: 1911-1922, 2020.
73. Zare A, Ahadi A, Larki P, Omrani MD, Zali MR, Alamdari NM and Ghaedi H: The clinical significance of miR-335, miR-124, miR-218 and miR-484 downregulation in gastric cancer. Mol Biol Rep 45: 1587-1595, 2018.
74. Liu J and Li SM: MiR-484 suppressed proliferation, migration, invasion and induced apoptosis of gastric cancer by targeting CCL-18. Int J Exp Pathol 101: 203-214, 2020.
75. Li Y, Liu Y, Yao J, LI R and Fan X: Downregulation of miR-484 is associated with poor prognosis and tumor progression of gastric cancer. Diagn Pathol 15: 25, 2020.
76. Wang L and Gong W: NOX4 regulates gastric cancer cell invasion and proliferation by increasing ferroptosis sensitivity through regulating ROS. Int Immunopharmacol 132: 112052, 2024.
77. Qi X, Zhang DH, Wu N, Xiao JH, Wang X and Ma W: ceRNA in cancer: Possible functions and clinical implications. J Med Genet 52: 710-718, 2015.
78. Zhang D, Yan H, Li H, Hao S, Zhuang Z, Liu M, Sun Q, Yang Y, Zhou M, Li K and Hang C: TGFβ-activated kinase 1 (TAK1) inhibition by 5Z-7-Oxozeaenol attenuates early brain injury after experimental subarachnoid Hemorrhage. J Biol Chem 290: 19900-19909, 2015.
79. Yang Y, Qiu Y, Tang M, Wu Z, Hu W and Chen C: Expression and function of transforming growth factor-β-activated protein kinase 1 in gastric cancer. Mol Med Rep 16: 3103-3110, 2017.
80. Ahn S, Brant R, Sharpe A, Dry JR, Hodgson DR, Kilgour E, Kim K, Kim ST, Park SH, Kang WK, *et al*: Correlation between MEK signature and Ras gene alteration in advanced gastric cancer. Oncotarget 8: 107492-107499, 2017.
81. Lee J, Kim ST, Kim K, Lee H, Kozarewa I, Mortimer PGS, Odegaard JI, Harrington EA, Lee J, Lee T, *et al*: Tumor genomic profiling guides patients with metastatic gastric cancer to targeted treatment: The VIKTORY umbrella trial. Cancer Discov 9: 1388-1405, 2019.
82. Liu Z and Xing M: Induction of sodium/iodide symporter (NIS) expression and radioiodine uptake in nonthyroid cancer cells. PLoS One 7: e31729, 2012.
83. Wu X, Zhou F, Cheng B, Tong G, Chen M, He L, Li Z, Yu S, Wang S and Lin L: Immune activity score to assess the prognosis, immunotherapy and chemotherapy response in gastric cancer and experimental validation. PeerJ 11: e16317, 2023.
84. Liu J, Zhang B, Zhang Y, Zhao H, Chen X, Zhong L and Shang D: Oxidative stress and autophagy-mediated immune patterns and tumor microenvironment infiltration characterization in gastric cancer. Aging (Albany NY) 15: 12513-12536, 2023.
85. Ajani JA, D'Amico TA, Bentrem DJ, Corvera CU, Das P, Enzinger PC, Enzler T, Gerdes H, Gibson MK, Grierson P, *et al*: Gastric cancer, version 2.2025, NCCN clinical practice guidelines in oncology. J Natl Compr Canc Netw 23: 169-191, 2025.
86. Dai C, Shen L, Jin W, Lv B, Liu P, Wang X, Yin Y, Fu Y, Liang L, Ma Z, *et al*: Physapubescin B enhances the sensitivity of gastric cancer cells to trametinib by inhibiting the STAT3 signaling pathway. Toxicol Appl Pharmacol 408: 115273, 2020.
87. Liu H, Yao Y, Zhang J and Li J: MEK inhibition overcomes everolimus resistance in gastric cancer. Cancer Chemother Pharmacol 85: 1079-1087, 2020.
88. Wang Z, Chen Y, Li X, Zhang Y, Zhao X, Zhou H, Lu X, Zhao L, Yuan Q, Shi Y, *et al*: Tegaserod maleate suppresses the growth of gastric cancer in vivo and in vitro by targeting MEK1/2. Cancers (Basel) 14: 3592, 2022.